Cell. Mol. Life Sci. 63 (2006) 1095–1105
1420-682X/06/101095-11
DOI 10.1007/s00018-005-5450-3
© Birkhäuser Verlag, Basel, 2006

Cellular and Molecular Life Sciences

Review

Hexameric molecular motors: P4 packaging ATPase unravels the mechanism

D. E. Kainov[a, *], R. Tuma[a] and E. J. Mancini[b]

[a] Institute of Biotechnology and Department of Biological and Environmental Sciences, Viikki Biocenter P. O. Box 65, University of Helsinki, Helsinki 00014 (Finland), Fax: +358 919159930, e-mail: dkainov@hotmail.com
[b] Division of Structural Biology, The Henry Wellcome Building for Genomic Medicine, Oxford University, Roosevelt Drive, Oxford OX3 7BN (United Kingdom)

Received 30 September 2005; received after revision 8 December 2005; accepted 27 December 2005
Online First 28 February 2006

Abstract. Genome packaging into an empty capsid is an essential step in the assembly of many complex viruses. In double-stranded RNA (dsRNA) bacteriophages of the *Cystoviridae* family this step is performed by a hexameric helicase P4 which is one of the simplest packaging motors found in nature. Biochemical and structural studies of P4 proteins have led to a surprising finding that these proteins bear mechanistic and structural similarities to a variety of the pervasive RecA/F1-ATPase-like motors that are involved in diverse biological functions. This review describes the role of P4 proteins in assembly, transcription and replication of dsRNA bacteriophages as it has emerged over the past decade while focusing on the most recent structural studies. The P4 mechanism is compared with the models proposed for the related hexameric motors.

Keywords. Genome packaging, RecA-like motor, hexameric helicase, dsRNA bacteriophage, virus assembly.

P4 is required for genome packaging into empty procapsid in cystoviruses

Genome packaging into viral capsids protects the nucleic acid from nuclease degradation within the host cell as well as outside. Two main strategies for packaging viral genomes have been described: (i) capsid assembly around the viral nucleic acid; (ii) filling of preformed capsid with a previously synthesized nucleic acid or a nucleic acid that is being synthesized during packaging (Fig. 1). The first, co-condensation, mechanism has been studied in detail for both helical and icosahedral single-stranded RNA (ssRNA) viruses [1–6].

The second mechanism is best understood for the double-stranded DNA (dsDNA) bacteriophage *Φ*29, whose portal protein together with the terminase enzyme and RNA serves as the packaging motor [7, 8, 14]. The complex contains three components: (i) the head-tail connector, a dodecamer of protein p10, attached to a unique fivefold prohead vertex [9, 10]; (ii) a multimeric ring of structural RNAs [7, 11]; and (iii) several copies of ATPase-gp16 [12]. Since the gp16 of *Φ*29 and terminases (nucleases that process genomic DNA concatemers) of related dsDNA bacteriophages have been shown to catalyse NTP hydrolysis *in vitro*, these proteins are thought to provide energy for the packaging reaction [13]. It has been suggested that the energy released from ATP hydrolysis is somehow transmitted from the transiently associated gp16 to the connector, which in turn performs unidirectional DNA translocation [9, 14]. A recent single molecule study on gp16 suggested that the force generation step is coupled to the release of inorganic phosphate [15]. The mechanism for energy transduction to the portal and the role of RNA in the process [16], however, remain speculative.

In vitro packaging of dsRNA viruses has been studied for bacteriophages of the *Cystoviridae* family [17–19]. The as-

* Corresponding author.

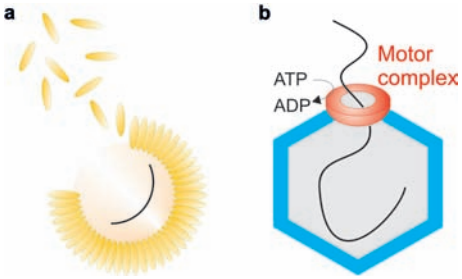

Figure 1. Two main strategies for packaging of viral genomes.(*a*) Capsid assembly around the viral genome. This strategy is typical for both helical and icosahedral viruses such as TMV, HIV, M13 and L-A. (*b*) Genome packaging into preformed capsid. A molecular motor uses energy from nucleotide triphosphate hydrolysis to translocate genomic precursors into a capsid precursor. This strategy is typical for icosahedral viruses, such as *Φ*29, adenovirus and *ϕ*6.

sembly of dsRNA bacteriophages proceeds via formation of procapsids followed by packaging, similarly to genome packaging in *Φ*29 and other dsDNA bacteriophages [20–23]. Bacteriophage *ϕ*6 is the prototype of the family *Cystoviridae*, which includes eight additional members (*ϕ*7–*ϕ*14) [17, 18]. *ϕ*6 exhibits sequence similarity to *ϕ*7, *ϕ*9, *ϕ*10, *ϕ*11 and *ϕ*13, while *ϕ*8 and *ϕ*12 are more distantly related [24–27]. Bacteriophage *ϕ*6 infects the plant pathogenic bacterium *Pseudomonas syringae* [28]. The *ϕ*6 virion consists of three sequential layers: a protein-lipid envelope, a nucleocapsid protein shell and inner icosahedral protein assembly (polymerase complex or PX) (Fig. 2a, and b). During virus entry the first two layers are sequentially removed and the PX is delivered into the cytoplasm [29]. PX is composed of 120 copies of the major structural protein P1 [30, 31], 12 monomers of RNA-dependent RNA polymerase P2 [32], 12 hexamers of packaging motor P4 [33, 34] and 30 dimers of assembly factor P7 [35]. P2 and P4 reside at the fivefold verices in the icosahedral PX [36, 37]. PX contains an ~13 kb genome comprising three segments: L, large; M, middle; and S, small [38, 39]. PX transcribes genome, synthesizing three (+)-strand RNAs that are extruded from the particle (Fig. 2c) [40]. These RNAs serve as templates for viral protein synthesis. Newly synthesized proteins P1, P2, P4 and P7 assemble into empty PX (procapsid) [22]. Procapsid packages each (+)-strand RNAs specifically [41]. The rate of RNA packaging was estimated at 2000 bases per minute [41]. Packaging specificity is determined by packaging signals, each of which encompasses about a 210–280 nucleotide-long stretch within the 5′ non-coding end of each segment. Packaging of the three RNA segments is sequential [19, 42]. Procapsid recognizes the three (+)-strand RNAs in a segment-specific manner and sequentially translocates the RNA molecules into the particle interior (Fig. 3a, d). Segment s+ is packaged first, followed by m+ and then l+ [41, 43]. PX undergoes considerable conformational changes during packaging [20]. Each ex-

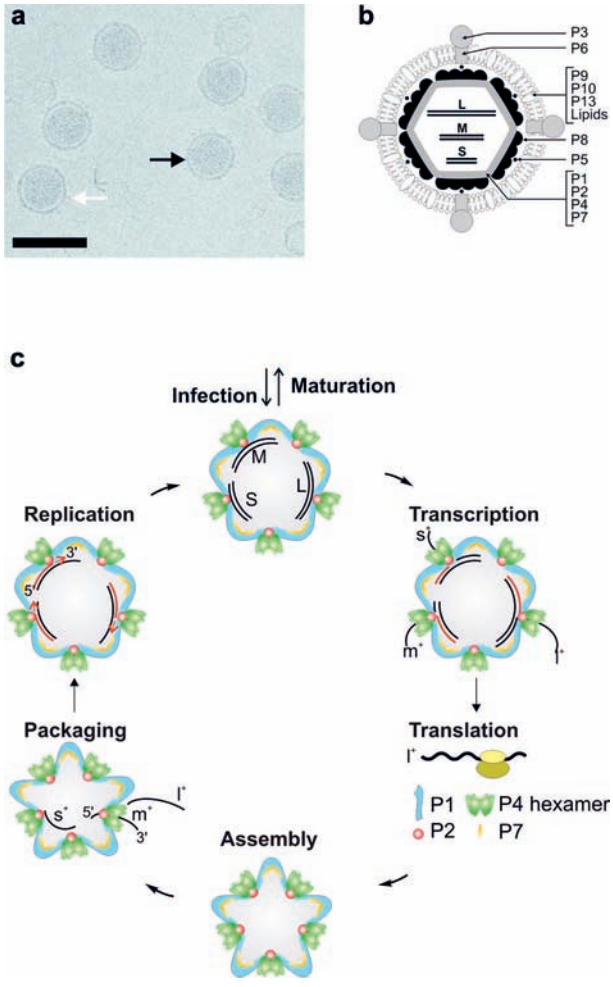

Figure 2. Structural organization and life cycle of *Cystoviridae*. (*a*) Electron cryo-micrograph of ϕ6 virion (~85 nm diameter). The virion membrane is clearly visible (black arrow) as are the external spikes (white arrow). The scale bar represents 100 nm [96]. (*b*) Diagram of *ϕ*6 virion [97]. Proteins P1, P2, P4 and P7 form the viral core, which occludes three dsRNA segments, L, M and S. A shell built from protein P8 covers the core. The P8-coated particle (nucleocapsid) is further enveloped with a lipid membrane, which contains proteins P9, P6, P10 and P13. P3, which is anchored to the viral membrane by P6, is the receptor-binding protein. Protein P5 is an endopeptidase residing between P8 shell and the membrane. (*c*) Simplified scheme of the cystoviral life cycle. During the host membrane penetration the viral membrane is shed, the P8 shell disassembles and the core becomes activated. dsRNA molecules are transcribed inside the core-producing mRNAs, which are extruded from the core. The mRNAs are translated using host cell ribosomes producing viral proteins. Viral proteins P1, P2, P4 and P7 assemble into a procapsid, and the (+)-strand RNAs are packaged into the procapsid through the central channel of the hexameric P4. Upon packaging the procapsid expands and replication is initiated. The dsRNA-filled particles can then enter additional rounds of transcription or mature into infectious virions. The latter pathway uses proteins produced by the translation of m^+ and s^+ ssRNA segments, which is followed by the acquisition of the rest of the viral structural proteins together with the lipid membrane (not shown). The mature virus particles are released by lysis of the host cell.

pansion event may also expose high-affinity RNA binding sites in a segment-specific fashion on the PX surface [41]. Estimates of the internal volume for the empty and filled PX showed that particle has to expand several times during ssRNA packaging in order to accommodate all three segments. The packaged (+)-RNA is then replicated inside the PX to yield genomic dsRNA [44, 45].

Protein P4 constitutes the packaging motor (Fig. 3a, b) [34]. P4 was first identified as the packaging NTPase of ϕ6 virus, since PX devoid of P4 was completely inactive in ssRNA packaging assays [47–49]. In addition, P4 acts as a passive conduit in semi-conservative transcription, when the newly synthesized messenger RNA (mRNA) molecules are extruded from PX by the action of P2 polymerase [50]. Furthermore, under defined *in vitro* conditions the assembly of empty PX is dependent on hexameric P4 [22, 51].

It is not clear whether other dsRNA viruses, in particular, members of the *Reoviridae* family, adopt a similar scheme for genome packaging. Molecular mechanisms of genome packaging in dsDNA viruses are poorly understood due to the complex nature of the packaging machinery, which consists of several transiently associated subunits [52–54]. In the following sections, we discuss recent biochemical and structural results that provided the first glimpse of the mechanism of nucleic acid packaging in atomic detail.

P4 is a hexameric packaging ATPase, structurally related to RecA/F1-ATPase-like motors

P4 enzymes from four cystoviruses (ϕ6, ϕ8, ϕ12 and ϕ13) were cloned, expressed and characterized (Table 1) [34, 51, 55–59]. P4 proteins belong to the F4 hexameric helicase family, also known as the DnaB-like family [60]. F4 helicases contain five conserved motifs (Fig. 4c) [61]. F4 helicases generally form hexameric ring structures, unwind DNA in the 5′ to 3′ direction, and often associate physically with DNA primases and function in DNA replication of bacteria and bacteriophages [62].

P4 proteins are hexameric, ssRNA-stimulated NTPases [34, 55, 56]. ϕ12 P4 exhibits strict specificity for purine nucleotide triphosphates, whereas P4 proteins from the other three bacteriophages hydrolyse both purines and

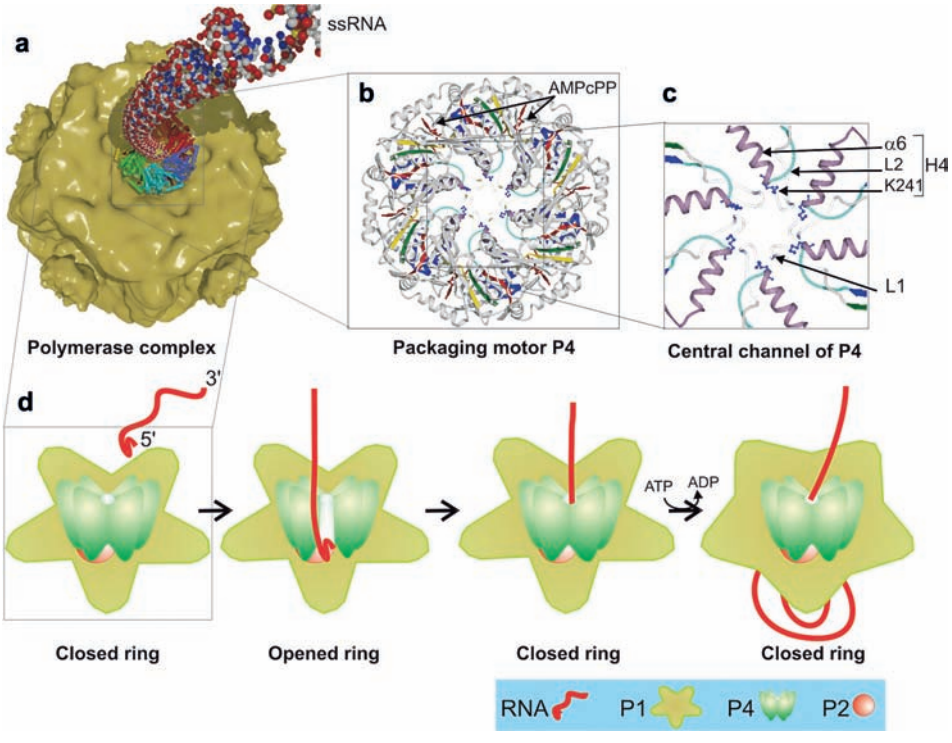

Figure 3. (*a*) The P4 hexameric motor in the act of packaging ssRNA into empty capsid. A 20 Å icosahedral reconstruction of ϕ6 procapsid (proteins P1, P2, P4 and P7) is shown in a yellow isosurface representation [36]. The density for one of the P4 turrets has been removed and substituted with a ribbon representation of the crystal structure of hexameric P4 from bacteriophage ϕ12 [63]. A modeled A-form ssRNA is shown (atom colors are carbon, white; oxygen, red; nitrogen, blue; phosphorus, yellow). (*b*) Enlarged ribbon representation of hexameric P4. Six AMPcPP molecules occupy nucleotide-binding sites on the interfaces between the subunits. (*c*) The central channel of P4 hexamer viewed from the C-terminal face (loops L1 and L2, and helix α6 are indicated). (*d*) Model of RNA loading into the packaging motor in the context of the viral shell (one fivefold vertex). From left to right: the packaging signal at the 5′ end of RNA is specifically recognized by the procapsid protein P1. RNA then binds to a putative primary binding site on the surface of the P4 and triggers ring opening of the hexamer. After closing, P4 processively translocates RNA into the procapsid, which concomitantly expands and exposes a binding site on P1 for the next RNA segment.

Table 1. Morphology and biochemical activities of isolated P4 proteins.

P4	ϕ6	ϕ8	ϕ12	ϕ13
Mol Weight (kDa)	35.0	34.1	35.1	37.6
Oligomerization state[1]	hexamer (+ATP/ADP)	hexamer	hexamer	hexamer
$K_{M(ATP)\ without}$ RNA, mM[1]	0.19 ± 0.05	ND[a]	1.5 ± 0.04	0.40 ± 0.05
$K_{M(ATP)\ with}$ polyC, mM[1]	ND	0.167 ± 0.01	0.49 ± 0.02	ND
ssRNA binding[1]	none	strong	none	strong
ssRNA translocation[1]	none	strong	weak	strong
COD activity[1]	none	strong	none	weak
Structure determination[2]	in progress	ND	2.0 Å, SAD	in progress

[1] Data from [55, 57, 58]
[2] For details see [63, 94, 95]
COD, complementary oligonucleotide displacement (similar to helicase activity); SAD, single-wavelength anomalous diffraction; ND, not determined; ND[a], not determined due to undetectable activity.

pyrimidines [50, 55]. P4 proteins from ϕ8 and ϕ13 efficiently bind RNA and possess RNA-specific helicase activity. P4 proteins from ϕ6 and ϕ12 have lower affinity for RNA and acquire the helicase activity only upon association with PX (Table 1). P4 proteins translocate ssRNA in the 5′ to 3′ direction [55].

The crystal structure of hexameric packaging enzyme P4 from bacteriophage ϕ12 has been solved [63]. Figure 4 shows a ribbon diagram of the P4 monomer. The triangular wedge-shaped monomer is composed of an N-terminal domain, a central conserved core and a C-terminal region. The sequence of the N-terminal domain is not conserved between different members of the *Cystoviridae* (Fig. 4c), and may be involved in functions other than RNA translocation. The first 40 residues of the N-terminal domain of ϕ12 P4 fold into a safety pin-like feature, which extends toward the neighboring subunit. This structural feature, also present in RepA and T7 helicase, could be involved in hexamer formation or stabilization. The central core, together with part of the C-terminal region, forms a Rossmann-type nucleotide-binding domain containing a twisted, eight-stranded β sheet of mixed parallel and antiparallel topology flanked by five helices. Despite negligible sequence similarity [63], the structure of the nucleotide-binding domain of P4 is strongly similar to the equivalent domain in RecA, the T7 helicase, the N-ethylmaleimide-sensitive fusion protein (NFS) and the bacterial conjugation protein TrwB. In addition, the nucleotide binding fold of P4 is strikingly similar to α and β subunits of F1-ATPase [63]. Terminase subunits from dsDNA phages and herpesvirus (U_L15 in HSV-1, gp17 in bacteriophage T4, gp16 in Φ29, gpP in P2, gpA in λ) were proposed to contain a similar RecA-like domain [64–70]. The C-terminal region encompasses a patch of nonconserved hydrophobic residues that are dispensable for hexamerization but essential for binding to the PX [71]. The structure of the C-terminal region is mostly disordered except for a short helix including residues 313–328, which is ordered in the pre-hydrolysis state (P4 ϕ12 in complex with AMPcPP and Mg^{2+}) and disordered in the post-hydrolysis state (P4 ϕ12 in complex with ADP and Mg^{2+}). Detailed mapping of the sites and nature of P4-PX interactions revealed that the C-terminal region is dynamically coupled to the RecA-like catalytic core [unpublished observation]. We propose that the C-terminal region undergoes a conformational change to shut off the activity after packaging [50].

Six P4 monomers form an almost perfectly symmetric hexamer enclosing a funnel-like central channel (Fig. 3b and 3c). This channel is occupied by a portion of helix α6 and two loops, L1 and L2, named by analogy with the loops in T7 helicase, RepA and RecA [72–75].

In order to unravel the packaging mechanism and to compare it with the known RecA-like motor mechanisms, structures of P4 ϕ12 hexamers in distinct nucleotide-binding states were determined (Fig. 5a, b) [63]. Depending on the nucleotide state, significant differences have been observed mostly within the RecA-like core. The RecA-like core consists of five conserved motifs that are essential for mechano-chemical coupling (H1, H1a, H2, H3, H4), i.e. for transduction of energy released by ATP hydrolysis into translocation along nucleic acids and unwinding (Fig. 4b, c) [60]. The motifs can be divided according to their structural and functional properties: (i) The primary function of motifs H1, H1a and H2 is NTP-Mg^{2+}/NDP-Mg^{2+} binding; (ii) H4 functions solely or primarily in oligonucleotide binding; (iii) H3 participates in

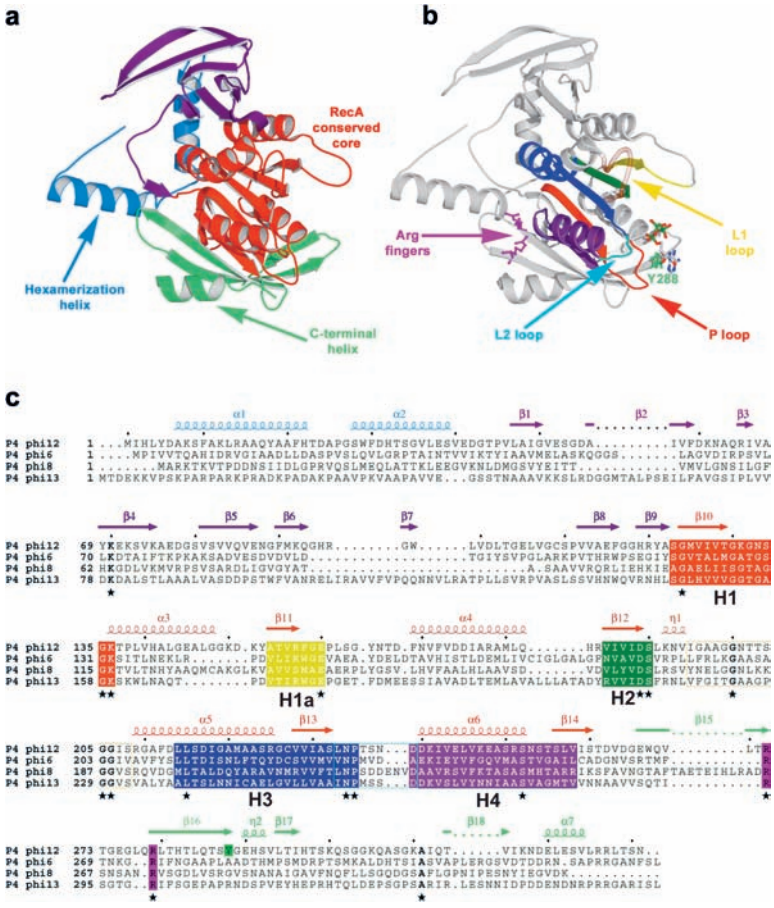

Figure 4. P4 monomers colored according to domain architecture (N-terminal, core, C-terminal, panel *a*) and according to the conserved helicase motifs (*b*) [60]. (*c*) Sequence alignment of cystoviral P4 proteins. Boxes, which indicate the conserved motifs of the RecA-like hexameric helicase family (H1, H1a, H2, H3, H4), are color-coded according to the same scheme as in panel (*b*). The positions of loops L1 (disordered) and L2 (ordered) are indicated. Secondary structure elements of ϕ12 P4 are shown above the aligned sequences and are color-coded according to the same scheme as in panel (*a*). Identical residues are marked with asterisk.

the molecular mechanism of coupling between ATP hydrolysis and translocation [62].

Nucleotide-binding site

Six equivalent nucleotide-binding pockets are located at the interfaces between adjacent subunits, close to the hexamer perimeter, some 25 Å from the central channel (Fig. 3b, 5d). In the substrate analog and the product-bound states all six nucleotide-binding pockets are occupied by the corresponding nucleotide. Four conserved residues (Lys136, Thr137, Glu160 and Asp189), belonging to H1, H1a and H2 motifs, line the binding pocket. Biochemical and structural analysis revealed that the corresponding residues of RecA/F1-ATPase-like motors play a role in triphosphate coordination, magnesium binding and ATP hydrolysis [76].

ϕ12 P4 is the only purine-specific NTPase among the P4 packaging enzymes. Purine specificity is conferred by three residues. The nucleotide base is sandwiched between Tyr288 from the catalytic subunit (i.e. the one providing residues of the H1, H1a and H2 motifs) and Gln278 from the neighboring subunit. Additionally, a hydrogen bond is established between the side chain of Ser292 and the N7 site of the adenine ring [63]. We proposed that these three residues are crucial for the correct positioning of the nucleotide within the binding pocket. Although these residues do not belong to the conserved helicase motifs, similar stacking interactions were found in RepA (Arg86 and Tyr243) and in T7 gp4 (Arg504 and Tyr535) [72, 73, 77].

RNA binding and loading

The P4 hexamer defines a portal channel of appropriate dimensions to accommodate ssRNA but not dsRNA. The central channel of the hexameric P4 is lined by the tips of helices α6 (motif H4) and two loops, L1 and L2 (Fig. 3c).

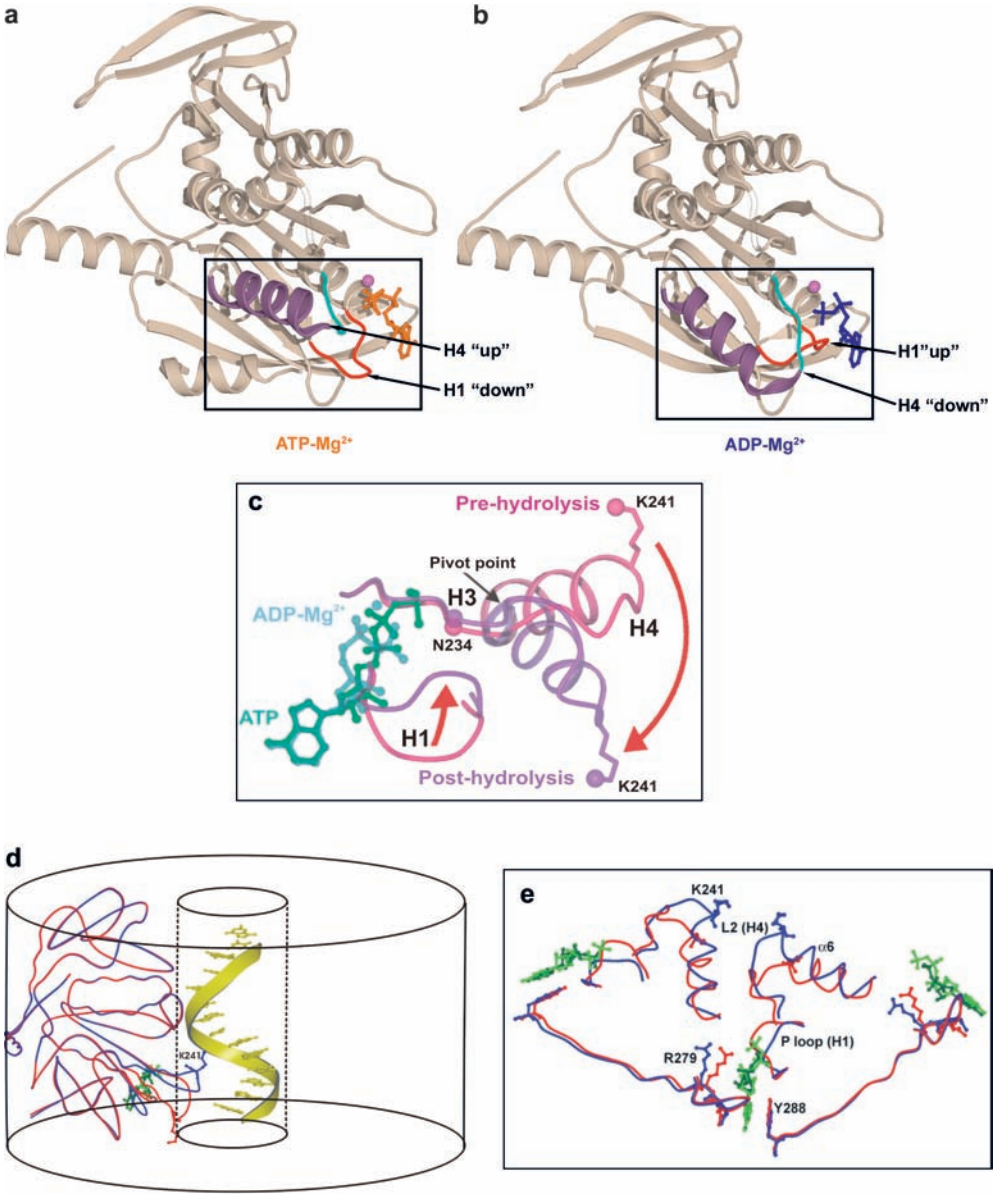

Figure 5. Conformational changes accompanying nucleotide hydrolysis. The structures of P4 in complex with AMPcPP-Mg^{2+} (*a*) and ADP-Mg^{2+} (*b*), respectively, are compared. (*c*) Details of conformational changes in the conserved motifs H1, H3 and H4. The red arrows indicate the conformational changes that the α6 helix-L2 loop (H3-H4) and P-loop (H1) undergo following ATP hydrolysis. (*d*) Backbone coil representation of one P4 subunit in the two distinct conformations (P4:AMPcPP-Mg^{2+} blue, P4:ADP-Mg^{2+} red) in the context of the hexamer (cylinder). Bound AMPcPP (green) and K241 are shown as ball-and-stick models. A-form ssRNA backbone is modeled as a ribbon running through the central channel. Stacked bases are shown in ball-and-stick. (*e*) Section through a dimer showing the conserved motifs together with arginine finger R279 and their conformational changes (color coding as in panel *d*). The Mg^{2+}, AMPcPP and ADP molecules are shown as ball-and-stick models.

RNA binding to ϕ12 P4 is weak [55], and consequently no stable complexes could be detected. It was not possible to co-crystallize ϕ12 P4 in the presence of oligonucleotides. However, RNA binding to the P4 motor confers catalytic cooperativity (increased Hill coefficient and decreased K_m) and stimulates hydrolysis (increased k_{cat}) [58]. These enzymatic signatures were used to assess the effect of mutations in L1 and L2 loops on RNA binding.

In ϕ8 P4, the L1 loop contains two lysine residues (Lys185 and Lys186). Mutation of the two lysines to alanine or deletion of the motif Leu-Lys-Lys completely abolished RNA binding, RNA-stimulated NTPase activity and translocation [78]. In ϕ12 P4, deletion of the corresponding portion of the L1 loop (Thr-Thr-Ser) completely inactivated the ATPase activity, despite the overall structure remaining essentially indistinguishable from that of wt [unpublished observation]. This result suggests that the

L1 loop might play a more active role in translocation than that of passive grommet, which constrains RNA to the center of the channel. One possibility is that the L1 loop helps to coordinate ATP hydrolysis with the RNA binding cycle.

Loop L2 lays between the H3 and H4 motifs. The N-terminal tip of α6 helix presents Lys241 to the central channel. Replacing Lys241 with Ala reduced RNA stimulation of ATP hydrolysis while leaving the overall structure unaffected. In contrast to wt protein, the K_m value of the mutant increased with the addition of ssRNA, whereas the Hill coefficient remained unchanged [unpublished results]. Thus it was concluded that the L1 and L2 loops are essential for RNA binding and translocation [78].

Given that ϕ8 P4 can bind circularly closed ssDNA, the intriguing question of how this is topologically accomplished, was raised. Hydrogen deuterium exchange (HDX) experiments [79] helped to resolve this issue. HDX visualized the hexamer dynamics associated with ATP hydrolysis and RNA translocation, creating an important link between time-resolved spectroscopic observations and the high-resolution structural snapshots of these molecular motors. HDX revealed a transition state associated with RNA loading, which proceeds via opening of the hexameric ring (Fig. 3d) [78]. The loading mechanism is similar to that of other hexameric helicases but does not require ATP binding or hydrolysis [80–82].

Coupling of ATP hydrolysis to RNA translocation

Comparison of P4 structures in relevant nucleotide bound states revealed that the H4 motif and the H1 motifs undergo major conformational changes as a consequence of ATP hydrolysis and phosphate release (Fig. 5) [63]. In the complex of P4 with a substrate analog (AMPcPP-Mg^{2+}), the P-loop is in a 'down' conformation (Fig. 5a), whereas in the product complex, it is in an 'up' conformation (Fig. 5b). This is accompanied by swiveling of the H4 region from an up position in the substrate complex to a down position in the product complex (Fig. 5c). We proposed that this movement is associated with an ~6 Å translocation of the RNA bound to Lys241 (Fig. 5d) [63].

In order to elucidate the nature and extent of the coupling between H4 (i.e. RNA translocation) and H1 regions and ATP hydrolysis a mutation (Lys241 to Cys) was introduced. This mutation reversibly cross-linked the L2 loops from neighboring subunits and effectively immobilized independent H4 region motion [unpublished observation]. Under non-reducing conditions, the mutant had no ATPase activity irrespective of the presence of RNA. In the presence of DTT, the disulfide bonds were cleaved and basal ATPase activity was restored. This suggested that the swiveling motion of H4 is essential for ATPase activity, possibly by aiding transition state formation during hydrolysis.

The conserved H3 motif was proposed to play a role in energy transduction [63]. Site-directed mutagenesis followed by biochemical and structural analysis revealed that the conserved Asn234 within H3, which is in close proximity to the γ-phosphate, relays exchange of bound nucleotide to conformational changes in the H4 region (Fig. 5c). Thus, Asn234 constitutes the γ-phosphate sensor that stabilizes the H4 in the up conformation in the ATP state, effectively driving the recoil stroke of the motor. In other hexameric helicases H3 motifs play the same role, sensing the γ-phosphate and propagating conformational changes from the nucleotide-binding site to residues in the DNA-binding motif H4 [74, 83, 84]. Hydrogen deuterium exchange in solution confirmed this mechanism for ϕ8 P4 [78].

Coordination of ATP hydrolysis between subunits

The coordination of ATP hydrolysis requires structural elements for communication between subunits. 'Arginine fingers', common features of multimeric ATPases, often perform this role. An arginine finger is contributed by a neighboring subunit to coordinate the γ-phosphate of the bound nucleotide [77, 84–87]. Arginine fingers contribute to NTP hydrolysis through stabilization of the transition state and may trigger conformational changes following hydrolysis [85, 88, 89]. Arg279 in ϕ12 P4 was proposed to mediate coordination of ATP hydrolysis among subunits (Fig. 5e) [63]. In the substrate bound state Arg279 is locked away from the nucleotide pocket by hydrogen bond to Arg251 within the H4 region. After hydrolysis the α6 helix (H4 region) swings down and disrupts the Arg251-Arg279 interaction. Consequently, Arg279 is released and inserted into the nucleotide-binding site of the neighboring subunit (Fig. 6c) [63].

Other residues belonging to the H3-H4 motifs have been shown to play crucial roles in hexameric motor mechanisms. For example, the arginine finger insertion in T7 helicase is dependent on the conformation of a conserved serine in the H3 motif [73, 90]. In P4, the hydroxyl group of Ser252 (in this case belonging to the motif H4) is adjacent to the γ-phosphate of the nucleotide bound in the active site of the neighboring subunit. We propose that Ser252 coordinates insertion of the arginine finger with the motion of H4 region.

We propose a model for the sequential ATP hydrolysis and mechano-chemical coupling mechanism (Fig. 6). In the first round (Fig. 6c), hydrolysis at Subunit 4 allows stochastic motion of H4 (and the bound RNA) which in turn inserts Arg279 into the active site of Subunit 3 and stabilizes the transition state. In the second round

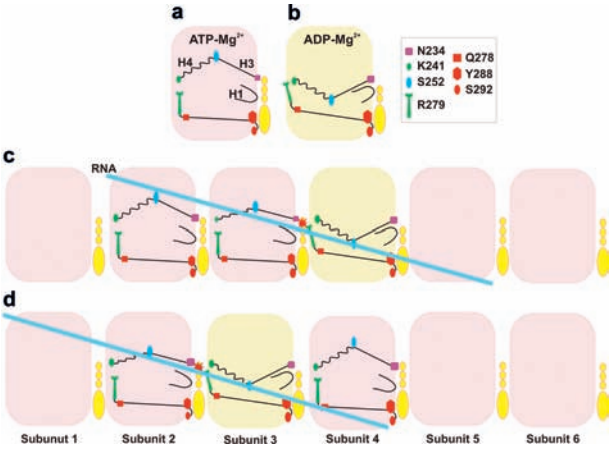

Figure 6. Model of sequential hydrolysis and RNA translocation by P4. (*a, b*) Schematic representation of the conserved motifs and position of important amino acid residues in the context of one ϕ12 P4 subunit together with a bound ATP (*a*) and ADP (*b*). The right panel shows residue and color keys. (*c*, *d*) Schematic description of the sequential hydrolysis coordination and RNA translocation within the hexamer. Two steps of the sequential mechanism are shown (*c* and *d*). The P4 hexamer is peeled open and viewed from inside the ring looking outward. The ATP-bound subunits are colored pink; the ADP-bound, yellow; the ssRNA, blue. Subunits 1, 5 and 6 adopt the ATP-bound conformation shown in (*a*); structural elements in the subunits are not shown. (*c*) Hydrolysis at Subunit 4 allows for motion of H4 motif (α6-L2 region) with the bound RNA to the preferred down position. This movement inserts the arginine finger R279 into the catalytic site of Subunit 3. This is required for transition state formation and hydrolysis at Subunit 3. (*d*) The cycle repeats at sites 2–3 while Subunit 4 binds ATP and H4 returns to its initial 'up' conformation. At this point RNA is already detached from this subunit.

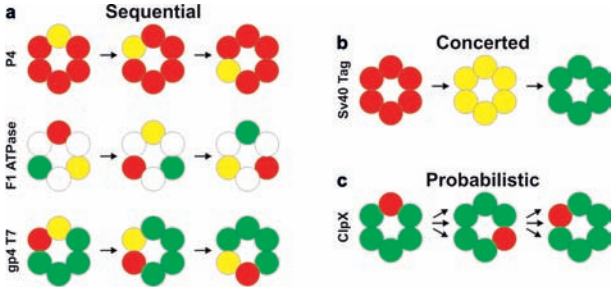

Figure 7. Alternative models for ATP hydrolysis and translocation in hexameric motors. (*a*) Sequential hydrolysis model, in which ATP hydrolysis in one subunit is followed sequentially by hydrolysis in the catalytic neighboring subunit and so on, was proposed for RecA-like hexameric motors from SFIII subfamily (T7gp4 helicase, [91]), F1-ATPase family [98] as well as P4 packaging ATPases [63]. (*b*) Concerted hydrolysis model, in which six subunits simultaneously bind and hydrolyse six ATPs, was proposed for SFIII and AAA$^+$ family members [92]. (*c*) Probabalistic hydrolysis model, in which any of the six subunits can independently hydrolyse ATP, was proposed for unfoldases from the AAA$^+$ subfamily, such as ClpX [93]. This protein in complex with peptidase powers protein unfolding and degradation. The trajectory of ATP hydrolysis within the hexameric ring of the ClpX is dictated by stochastic interactions with the translocated polypeptide. The red (ATP), yellow (ADP or ADP ± P_i) and green (empty) circles represent unique catalytic subunits on the hexamer while the white circles represent non-catalytic sites.

(Fig. 6d), hydrolysis and phosphate release proceed at Subunit 3, and the catalytic cycle is repeated at Subunit 2. Subunit 4 then returns to the initial, ATP-bound, state.

In the presence of RNA, ATP hydrolysis becomes sequential and apparently cooperative. In contrast to other cooperative enzymes, cooperativity in P4 is a result of coordinated hydrolysis rather than modulation of ATP affinity among subunits [57, 58]. Structurally, this could be explained by correlated motion of two neighboring H4 regions that are simultaneously bound to RNA. In effect, RNA acts as a stress loop which temporary stores energy between individual steps.

Several other Rec-A like hexameric motors share the sequential mechanism. A helicase domain gp4D from bacteriophage T7 is the closest structural relative of ϕ12 P4 [73]. A deterministic sequential hydrolysis model [91] is similar to that of P4 except for the stochastic features in the latter (Fig. 7a). F1-ATPase shares similar sequential mechanism of hydrolysis except that only every other subunit is active (Fig. 7a). In contrast to the sequential mechanism several other hexameric motors adopt different reaction schemes. For example, it has been proposed that SV40 large T-antigen hydrolyses ATP in a concerted fashion (Fig. 7b) [92], while the subunits of ClpX unfoldase operate independently (Fig. 7c) [93].

Future directions

Helicases bind DNA or RNA irrespective of the sequence. However, most of these motors are able to discern between ssDNA and ssRNA, which suggests that they are able to probe subtle differences of the nucleic acid backbone. For example, ϕ8 P4 hexamer binds ssDNA but translocates only along ssRNA [55]. The specific mode of binding and properties of the nucleic acid backbone play an important role in the mechanism. Thus, it is important to determine the structure of P4 with a bound oligonucleotide substrate.

Structure determination of P4 proteins from related cystoviruses provides a new avenue for comparative studies and evolutionary insights. In addition, comparison of structural and biochemical properties can delineate which mechanistic features are conserved among all P4 proteins and which are specific to each virus. The conserved mechanistic principles might be shared with other oligomeric molecular motors.

As demonstrated recently for the dsDNA packaging motor, single-molecule studies can provide the necessary experimental data to test the proposed P4 packaging model [15]. Preliminary data suggest that it is possible to immobilize individual hexamers and observe translocation rates using an engineered RNA substrate. This approach

will be extended to the P4 motor in the context of viral procapsid.

Acknowledgements. Andrey Golubtsov is thanked for critical reading of the manuscript. Work was supported by the Human Frontiers Science Programme, the UK Medical Council and the Academy of Finland (Finnish Centre of Excellence Program 2000–2005, and grant 1206926, R. T.). D. E.K. is a fellow of the Finnish National Graduate School in Informational and Structural Biology. E. J.M. was supported by an EMBO postdoctoral fellowship (ALTF-192) and HFSP.

1 Beckett D., Wu H. N. and Uhlenbeck O. C. (1988) Roles of operator and non-operator RNA sequences in bacteriophage R17 capsid assembly. J. Mol. Biol. **204:** 939–947
2 Berkowitz R., Fisher J. and Goff S. P. (1996) RNA packaging. Curr. Top. Microbiol. Immunol. **214:** 177–218
3 Buck K. W. (1999) Replication of tobacco mosaic virus RNA. Philos. Trans. R. Soc. Lond. B Biol. Sci. **354:** 613–627
4 Fujimura T., Esteban R., Esteban L. M. and Wickner R. B. (1990) Portable encapsidation signal of the L-A double-stranded RNA virus of S. cerevisiae. Cell **62:** 819–828
5 Russell R. S., Liang C. and Wainberg M. A. (2004) Is HIV-1 RNA dimerization a prerequisite for packaging? Yes, no, probably? Retrovirology **1:** 23
6 Valegard K., Murray J. B., Stockley P. G., Stonehouse N. J. and Liljas L. (1994) Crystal structure of an RNA bacteriophage coat protein-operator complex. Nature **371:** 623–626
7 Hendrix R. W. (1998) Bacteriophage DNA packaging: RNA gears in a DNA transport machine. Cell **94:** 147–150
8 Grimes S., Jardine P. J. and Anderson D. (2002) Bacteriophage phi 29 DNA packaging. Adv. Virus Res. **58:** 255–294
9 Simpson A. A., Tao Y., Leiman P. G., Badasso M. O., He Y., Jardine P. J. et al. (2000) Structure of the bacteriophage phi29 DNA packaging motor. Nature **408:** 745–750
10 Morais M. C., Choi K. H., Koti J. S., Chipman P. R., Anderson D. L. and Rossmann M. G. (2005) Conservation of the capsid structure in tailed dsDNA bacteriophages: the pseudoatomic structure of phi29. Mol. Cell **18:** 149–159
11 Guo P., Grimes S. and Anderson D. (1986) A defined system for *in vitro* packaging of DNA-gp3 of the Bacillus subtilis bacteriophage phi 29. Proc. Natl. Acad. Sci. USA **83:** 3505–3509
12 Guo P., Peterson C. and Anderson D. (1987) Prohead and DNA-gp3-dependent ATPase activity of the DNA packaging protein gp16 of bacteriophage phi 29. J. Mol. Biol. **197:** 229–236
13 Ibarra B., Valpuesta J. M. and Carrascosa J. L. (2001) Purification and functional characterization of p16, the ATPase of the bacteriophage Phi29 packaging machinery. Nucleic Acids Res. **29:** 4264–4273
14 Guo P. (2002) Structure and function of phi29 hexameric RNA that drives the viral DNA packaging motor: review. Prog. Nucleic Acid Res. Mol. Biol. **72:** 415–472
15 Chemla Y. R., Aathavan K., Michaelis J., Grimes S., Jardine P. J., Anderson D. L. et al. (2005) Mechanism of force generation of a viral DNA packaging motor. Cell **122:** 683–692
16 Chen C. and Guo P. (1997) Sequential action of six virus-encoded DNA-packaging RNAs during phage phi29 genomic DNA translocation. J. Virol. **71:** 3864–3871
17 Mindich L. (1999) Precise packaging of the three genomic segments of the double-stranded-RNA bacteriophage phi6. Microbiol Mol Biol Rev **63:** 149–160
18 Mindich L. (2004) Packaging, replication and recombination of the segmented genome of bacteriophage Phi6 and its relatives. Virus Res. **101:** 83–92
19 Sun Y., Qiao X., Qiao J., Onodera S. and Mindich L. (2003) Unique properties of the inner core of bacteriophage phi8, a virus with a segmented dsRNA genome. Virology **308:** 354–361
20 Butcher S. J., Dokland T., Ojala P. M., Bamford D. H. and Fuller S. D. (1997) Intermediates in the assembly pathway of the double-stranded RNA virus phi6. EMBO J. **16:** 4477–4487
21 Olkkonen V. M., Gottlieb P., Strassman J., Qiao X. Y., Bamford D. H. and Mindich L. (1990) *In vitro* assembly of infectious nucleocapsids of bacteriophage phi 6: formation of a recombinant double-stranded RNA virus. Proc. Natl. Acad. Sci. USA **87:** 9173–9177
22 Poranen M. M., Paatero A. O., Tuma R. and Bamford D. H. (2001) Self-assembly of a viral molecular machine from purified protein and RNA constituents. Mol. Cell **7:** 845–854
23 Poranen M. M. and Tuma R. (2004) Self-assembly of double-stranded RNA bacteriophages. Virus Res. **101:** 93–100
24 Gottlieb P., Potgieter C., Wei H. and Toporovsky I. (2002) Characterization of phi12, a bacteriophage related to phi6: nucleotide sequence of the large double-stranded RNA. Virology **295:** 266–271
25 Hoogstraten D., Qiao X., Sun Y., Hu A., Onodera S. and Mindich L. (2000) Characterization of phi8, a bacteriophage containing three double-stranded RNA genomic segments and distantly related to Phi6. Virology **272:** 218–224
26 Mindich L., Qiao X., Qiao J., Onodera S., Romantschuk M. and Hoogstraten D. (1999) Isolation of additional bacteriophages with genomes of segmented double-stranded RNA. J. Bacteriol **181:** 4505–4508
27 Qiao X., Qiao J., Onodera S. and Mindich L. (2000) Characterization of phi 13, a bacteriophage related to phi 6 and containing three dsRNA genomic segments. Virology **275:** 218–224
28 Semancik J. S., Vidaver A. K., Van Etten J. L. (1973) Characterization of segmented double-helical RNA from bacteriophage phi6. J. Mol. Biol. **78:** 617–625
29 Bamford D. H., Palva E. T. and Lounatmaa K. (1976) Ultrastructure and life cycle of the lipid-containing bacteriophage phi 6. J. Gen. Virol. **32:** 249–259
30 Ktistakis N. T. and Lang D. (1987) The dodecahedral framework of the bacteriophage phi 6 nucleocapsid is composed of protein P1. J. Virol. **61:** 2621–2623
31 Steely H. T. Jr, Lang D. (1984) Electron microscopy of bacteriophage phi 6 nucleocapsid: two-dimensional image analysis. J. Virol. **51:** 479–483
32 Makeyev E. V. and Grimes J. M. (2004) RNA-dependent RNA polymerases of dsRNA bacteriophages. Virus Res. **101:** 45–55
33 Gottlieb P., Strassman J. and Mindich L. (1992) Protein P4 of the bacteriophage phi 6 procapsid has a nucleoside triphosphate-binding site with associated nucleoside triphosphate phosphohydrolase activity. J. Virol. **66:** 6220–6222
34 Juuti J. T., Bamford D. H., Tuma R., Thomas G. J. Jr (1998) Structure and NTPase activity of the RNA-translocating protein (P4) of bacteriophage phi 6. J. Mol. Biol. **279:** 347–359
35 Juuti J. T. and Bamford D. H. (1997) Protein P7 of phage phi6 RNA polymerase complex, acquiring of RNA packaging activity by *in vitro* assembly of the purified protein onto deficient particles. J. Mol. Biol. **266:** 891–900
36 de Haas F., Paatero A. O., Mindich L., Bamford D. H. and Fuller S. D. (1999) A symmetry mismatch at the site of RNA packaging in the polymerase complex of dsRNA bacteriophage phi6. J. Mol. Biol. **294:** 357–372
37 Ikonen T., Kainov D., Timmins P., Serimaa R. and Tuma R. (2003) Locating the minor components of double-stranded RNA bacteriophage phi 6 by neutron scattering. J. Appl. Cryst. **36:** 525–529
38 Emori Y., Iba H. and Okada Y. (1980) Assignment of viral proteins to the three double-stranded RNA segments of bacteriophage phi6 genome: translation of phi 6 messenger RNAs transcribed *in vitro*. Mol. Gen. Genet. **180:** 385–389
39 Emori Y., Iba H. and Okada Y. (1982) Morphogenetic pathway of bacteriophage phi 6. A flow analysis of subviral and viral particles in infected cells. J. Mol. Biol. **154:** 287–310

40 Ewen M. E. and Revel H. R. (1988) *In vitro* replication and transcription of the segmented double-stranded RNA bacteriophage phi 6. Virology **165:** 489–498
41 Frilander M. and Bamford D. H. (1995) *In vitro* packaging of the single-stranded RNA genomic precursors of the segmented double-stranded RNA bacteriophage phi 6: the three segments modulate each other's packaging efficiency. J. Mol. Biol. **246:** 418–428
42 Qiao X., Casini G., Qiao J. and Mindich L. (1995) *In vitro* packaging of individual genomic segments of bacteriophage phi 6 RNA: serial dependence relationships. J. Virol. **69:** 2926–2931
43 Qiao X., Qiao J. and Mindich L. (1997) Stoichiometric packaging of the three genomic segments of double-stranded RNA bacteriophage phi6. Proc. Natl. Acad. Sci. USA **94:** 4074–4079
44 Frilander M., Gottlieb P., Strassman J., Bamford D. H. and Mindich L. (1992) Dependence of minus-strand synthesis on complete genomic packaging in the double-stranded RNA bacteriophage phi 6. J. Virol. **66:** 5013–5017
45 Gottlieb P., Strassman J., Frucht A., Qiao X. Y. and Mindich L. (1991) *In vitro* packaging of the bacteriophage phi6 ssRNA genomic precursors. Virology **181:** 589–594
46 Butcher S. J., Grimes J. M., Makeyev E. V., Bamford D. H. and Stuart D. I. (2001) A mechanism for initiating RNA-dependent RNA polymerization. Nature **410:** 235–240
47 Ewen M. E. and Revel H. R. (1990) RNA-protein complexes responsible for replication and transcription of the double-stranded RNA bacteriophage phi6. Virology **178:** 509–519
48 Juuti J. T. and Bamford D. H. (1995) RNA binding, packaging and polymerase activities of the different incomplete polymerase complex particles of dsRNA bacteriophage phi6. J. Mol. Biol. **249:** 545–554
49 Ojala P. M., Juuti J. T. and Bamford D. H. (1993) Protein P4 of double-stranded RNA bacteriophage phi 6 is accessible on the nucleocapsid surface: epitope mapping and orientation of the protein. J. Virol. **67:** 2879–2886
50 Kainov D. E., Lisal J., Bamford D. H. and Tuma R. (2004) Packaging motor from double-stranded RNA bacteriophage phi12 acts as an obligatory passive conduit during transcription. Nucleic Acids Res. **32:** 3515–3521
51 Kainov D. E., Butcher S. J., Bamford D. H. and Tuma R. (2003) Conserved intermediates on the assembly pathway of double-stranded RNA bacteriophages. J. Mol. Biol. **328:** 791–804
52 Catalano C. E., Cue D. and Feiss M. (1995) Virus DNA packaging: the strategy used by phage lambda. Mol. Microbiol. **16:** 1075–1086
53 Beard P. M. and Baines J. D. (2004) The DNA cleavage and packaging protein encoded by the UL33 gene of herpes simplex virus 1 associates with capsids. Virology **324:** 475–482
54 Newcomb W. W., Juhas R. M., Thomsen D. R., Homa F. L., Burch A. D., Weller S. K. et al. (2001) The UL6 gene product forms the portal for entry of DNA into the herpes simplex virus capsid. J. Virol. **75:** 10923–10932
55 Kainov D. E., Pirttimaa M., Tuma R., Butcher S. J., Thomas G. J. Jr, Bamford D. H. et al. (2003) RNA packaging device of double-stranded RNA bacteriophages, possibly as simple as hexamer of P4 protein. J. Biol. Chem. **278:** 48084–48091
56 Kainov D. E., Simonov V., Bamford D. H., Tuma R., Gottlieb P., Wei H. et al. (2004) Crystallization and preliminary X-ray diffraction analysis of bacteriophage phi12 packaging factor P7. Acta Crystallogr. D Biol. Crystallogr. **60:** 2368–2370
57 Lisal J., Kainov D. E., Bamford D. H., Thomas G. J. Jr, Tuma R. (2004) Enzymatic mechanism of RNA translocation in double-stranded RNA bacteriophages. J. Biol. Chem. **279:** 1343–1350
58 Lisal J. and Tuma R. (2005) Cooperative mechanism of RNA packaging motor. J. Biol. Chem. **280:** 23157–23164
59 Paatero A. O., Syvaoja J. E. and Bamford D. H. (1995) Double-stranded RNA bacteriophage phi 6 protein P4 is an unspecific nucleoside triphosphatase activated by calcium ions. J. Virol. **69:** 6729–6734
60 Hall M. C. and Matson S. W. (1999) Helicase motifs: the engine that powers DNA unwinding. Mol. Microbiol. **34:** 867–877
61 Ilyina T. V., Gorbalenya A. E. and Koonin E. V. (1992) Organization and evolution of bacterial and bacteriophage primase-helicase systems. J. Mol. Evol. **34:** 351–357
62 Caruthers J. M. and McKay D. B. (2002) Helicase structure and mechanism. Curr. Opin. Struct. Biol. **12:** 123–133
63 Mancini E. J., Kainov D. E., Grimes J. M., Tuma R., Bamford D. H. and Stuart D. I. (2004) Atomic snapshots of an RNA packaging motor reveal conformational changes linking ATP hydrolysis to RNA translocation. Cell **118:** 743–755
64 Bain D. L., Berton N., Ortega M., Baran J., Yang Q. and Catalano C. E. (2001) Biophysical characterization of the DNA binding domain of gpNu1, a viral DNA packaging protein. J. Biol. Chem. **276:** 20175–20181
65 Catalano C. E. (2000) The terminase enzyme from bacteriophage lambda: a DNA-packaging machine. Cell. Mol. Life Sci. **57:** 128–148
66 Goetzinger K. R. and Rao V. B. (2003) Defining the ATPase center of bacteriophage T4 DNA packaging machine: requirement for a catalytic glutamate residue in the large terminase protein gp17. J. Mol. Biol. **331:** 139–154
67 Guo P. (2005) Bacterial virus phi29 DNA-packaging motor and its potential applications in gene therapy and nanotechnology. Methods. Mol. Biol. **300:** 285–324
68 Linderoth N. A., Ziermann R., Haggard-Ljungquist E., Christie G. E. and Calendar R. (1991) Nucleotide sequence of the DNA packaging and capsid synthesis genes of bacteriophage P2. Nucleic Acids Res. **19:** 7207–7214
69 Przech A. J., Yu D. and Weller S. K. (2003) Point mutations in exon I of the herpes simplex virus putative terminase subunit, UL15, indicate that the most conserved residues are essential for cleavage and packaging. J. Virol. **77:** 9613–9621
70 White C. A., Stow N. D., Patel A. H., Hughes M. and Preston V. G. (2003) Herpes simplex virus type 1 portal protein UL6 interacts with the putative terminase subunits UL15 and UL28. J. Virol. **77:** 6351–6358
71 Paatero A. O., Mindich L. and Bamford D. H. (1998) Mutational analysis of the role of nucleoside triphosphatase P4 in the assembly of the RNA polymerase complex of bacteriophage phi6. J. Virol. **72:** 10058–10065
72 Niedenzu T., Roleke D., Bains G., Scherzinger E. and Saenger W. (2001) Crystal structure of the hexameric replicative helicase RepA of plasmid RSF1010. J. Mol. Biol. **306:** 479–487
73 Singleton M. R., Sawaya M. R., Ellenberger T. and Wigley D. B. (2000) Crystal structure of T7 gene 4 ring helicase indicates a mechanism for sequential hydrolysis of nucleotides. Cell **101:** 589–600
74 Story R. M. and Steitz T. A. (1992) Structure of the recA protein-ADP complex. Nature **355:** 374–376
75 Story R. M., Weber I. T. and Steitz T. A. (1992) The structure of the E. coli recA protein monomer and polymer. Nature **355:** 318–325
76 Walker J. E., Saraste M., Runswick M. J. and Gay N. J. (1982) Distantly related sequences in the alpha- and beta-subunits of ATP synthase, myosin, kinases and other ATP-requiring enzymes and a common nucleotide binding fold. EMBO J. **1:** 945–951
77 Ziegelin G., Niedenzu T., Lurz R., Saenger W. and Lanka E. (2003) Hexameric RSF1010 helicase RepA: the structural and functional importance of single amino acid residues. Nucleic Acids Res. **31:** 5917–5929
78 Lisal J., Lam T. T., Kainov D. E., Emmett M. R., Marshall A. G. and Tuma R. (2005) Functional visualization of viral molecular motor by hydrogen-deuterium exchange reveals transient states. Nat. Struct. Mol. Biol. **12:** 460–466
79 Lanman J., Prevelige P. E. Jr (2004) High-sensitivity mass spectrometry for imaging subunit interactions: hydrogen/deuterium exchange. Curr. Opin. Struct. Biol. **14:** 181–188

80 Ahnert P., Picha K. M. and Patel S. S. (2000) A ring-opening mechanism for DNA binding in the central channel of the T7 helicase-primase protein. EMBO J. **19:** 3418–3427
81 Richardson J. P. (2003) Loading Rho to terminate transcription. Cell **114:** 157–159
82 Skordalakes E. and Berger J. M. (2003) Structure of the Rho transcription terminator: mechanism of mRNA recognition and helicase loading. Cell **114:** 135–146
83 Datta S., Larkin C. and Schildbach J. F. (2003) Structural insights into single-stranded DNA binding and cleavage by F factor TraI. Structure (Camb) **11:** 1369–1379
84 Sawaya M. R., Guo S., Tabor S., Richardson C. C. and Ellenberger T. (1999) Crystal structure of the helicase domain from the replicative helicase-primase of bacteriophage T7. Cell **99:** 167–177
85 Soga S., Noumi T., Takeyama M., Maeda M. and Futai M. (1989) Mutational replacements of conserved amino acid residues in the alpha subunit change the catalytic properties of Escherichia coli F1-ATPase. Arch. Biochem. Biophys. **268:** 643–648
86 Crampton D. J., Guo S., Johnson D. E. and Richardson C. C. (2004) The arginine finger of bacteriophage T7 gene 4 helicase: role in energy coupling. Proc. Natl. Acad. Sci. USA **101:** 4373–4378
87 Hishida T., Han Y. W., Fujimoto S., Iwasaki H. and Shinagawa H. (2004) Direct evidence that a conserved arginine in RuvB AAA+ ATPase acts as an allosteric effector for the ATPase activity of the adjacent subunit in a hexamer. Proc. Natl. Acad. Sci. USA **101:** 9573–9577
88 Miwa Y., Horiguchi T. and Shigesada K. (1995) Structural and functional dissections of transcription termination factor rho by random mutagenesis. J. Mol. Biol. **254:** 815–837
89 Karata K., Inagawa T., Wilkinson A. J., Tatsuta T. and Ogura T. (1999) Dissecting the role of a conserved motif (the second region of homology) in the AAA family of ATPases. Site-directed mutagenesis of the ATP-dependent protease FtsH. J. Biol. Chem. **274:** 26225–26232
90 Washington M. T., Rosenberg A. H., Griffin K., Studier F. W. and Patel S. S. (1996) Biochemical analysis of mutant T7 primase/helicase proteins defective in DNA binding, nucleotide hydrolysis, and the coupling of hydrolysis with DNA unwinding. J. Biol. Chem. **271:** 26825–26834
91 Liao J. C., Jeong Y. J., Kim D. E., Patel S. S. and Oster G. (2005) Mechanochemistry of T7 DNA helicase. J. Mol. Biol. **350:** 452–475
92 Gai D., Zhao R., Li D., Finkielstein C. V. and Chen X. S. (2004) Mechanisms of conformational change for a replicative hexameric helicase of SV40 large tumor antigen. Cell **119:** 47–60
93 Martin A., Baker T. A. and Sauer R. T. (2005) Rebuilt AAA + motors reveal operating principles for ATP-fuelled machines. Nature **437:** 1115–1120
94 Mancini E. J., Grimes J. M., Malby R., Sutton G. C., Kainov D. E., Juuti J. T. et al. (2003) Order and disorder in crystals of hexameric NTPases from dsRNA bacteriophages. Acta. Crystallogr. D. Biol. Crystallogr. **59:** 2337–2341
95 Meier C., Mancini E. J., Bamford D. H., Walsh M. A., Stuart D. I. and Grimes J. M. (2005) Overcoming the false-minima problem in direct methods: structure determination of the packaging enzyme P4 from bacteriophage phi13. Acta Crystallogr. D Biol. Crystallogr. **61:** 1238–1244
96 Yang H., Makeyev E. V., Butcher S. J., Gaidelyte A. and Bamford D. H. (2003) Two distinct mechanisms ensure transcriptional polarity in double-stranded RNA bacteriophages. J. Virol. **77:** 1195–1203
97 Mindich L. and Bamford D. H. (1988) Lipid-containing bacteriophages. In: The Bacteriophages, pp. 475–520, Calendar R. (ed.), Plenum, New York
98 Boyer P. D. (1997) The ATP synthase-a splendid molecular machine. Annu. Rev. Biochem. **66:** 717–749


To access this journal online:
http://www.birkhauser.ch